Click Here for Full Article

Measurement of the connectivity of runoff source areas as determined by vegetation pattern and topography: A tool for assessing potential water and soil losses in drylands

Ángeles G. Mayor,[1] Susana Bautista,[1] Eric E. Small,[2] Mike Dixon,[3] and Juan Bellot[1]

[1] The connectivity of runoff sources is considered one of the main factors controlling the hydrology of sparsely vegetated landscapes. However, the empirical demonstration of this role is very limited, partly because of the scarcity of suitable connectivity metrics. In this work, we derived and tested a spatial metric, Flowlength, for quantifying the connectivity of runoff source areas considering both vegetation pattern and topography. Flowlength is calculated as the average of the runoff pathway lengths from all the cells in a raster-based map of the target site. We evaluated the relationships between the connectivity of runoff sources, measured with Flowlength, and the runoff and sediment yields from six plots and three catchments in semiarid southeast Spain. Flowlength distinguished varying degrees of connectivity between differing vegetation patterns with similar vegetation cover. The connectivity increased with the grain size of the bare areas and was positively related to plot runoff and sediment yields. Flowlength also correctly ranked the three catchments according to total runoff yielded during the study period. The inclusion of microtopographic information in the quantification of Flowlength improved the relationships between the pattern of runoff sources and the measured fluxes, highlighting the importance of topographic features in the connectivity of surface flows. In general, the microtopography had a net decreasing effect on the connectivity, which was mainly attributed to an increase in the amount of runoff sink areas caused by the sediment terracettes developed upslope of plants. Our results confirm that the connectivity of runoff sources is a key factor controlling runoff and erosion in semiarid lands and support the potential of Flowlength as a surrogate for the hydrological functioning of ecosystems with patchy vegetation.

1. Introduction

[2] The spatial structure of the vegetation in semiarid landscapes is commonly described as a source-sink system, with bare soil and vegetation patches acting, respectively, as sources and sinks of vital resources. This structure affects the retention of water and nutrients [*Ludwig and Tongway*, 1995; *Cerdà*, 1997; *Puigdefábregas et al.*, 1999; *Reid et al.*, 1999; *Schlesinger et al.*, 1999], which has implications in other ecosystem processes such as primary productivity [*Aguiar and Sala*, 1999].

[3] During the last decade, numerous field observations from semiarid areas worldwide have pointed to the importance of the vegetation pattern and the connectivity of runoff source areas in controlling hillslope runoff and sediment yields [*Abrahams et al.*, 1995; *Nicolau et al.*, 1996; *Bergkamp*, 1998; *Wainwright et al.*, 2000; *Wu et al.*, 2000; *Cammeraat*, 2002; *Boix-Fayos et al.*, 2006]. Indeed, the positive influence of the connectivity of runoff source areas on the transmission of surface runoff in semiarid environments has been implicitly or explicitly considered in several conceptual frameworks. Thus, for example, according to the conceptual model of soil loss developed by *Davenport et al.* [1998] for piñon-juniper ecosystems in western USA, the sharp increase of the erosion rate when cover is decreased beyond a threshold is related to the probability of runoff source areas being connected. This model was based on percolation theory [*Stauffer*, 1985; *Gardner et al.*, 1992], which assumes that critical threshold values of space occupation drive to sharp changes in connectivity. However, despite consensus about the important role of plant spatial pattern and the connectivity of runoff source areas in the hydrological functioning of semiarid environments, empirical support for this role is still very limited [*Wainwright et al.*, 2000; *Bautista et al.*, 2007].

[4] The connectivity of runoff source areas can be described at different spatial scales. At the broadest scale it

[1]Departamento de Ecología, Universidad de Alicante, Alicante, Spain.
[2]Department of Geology, University of Colorado, Boulder, Colorado, USA.
[3]Foothills Laboratory, University Corporation for Atmospheric Research, Boulder, Colorado, USA.

refers to the connectivity to the main channel of the different response units (areas with similar hydrological response) identified in a hillslope or catchment, while at the finest scale it is related to the connectivity of bare soil interpatches within the hillslope [*Cammeraat*, 2002; *Kirkby et al.*, 2002; *Vanacker et al.*, 2005]. In this paper, we focus on the study of connectivity at this latter scale.

[5] The loss of potential connectivity of the bare soil areas on a hillslope may be produced by any physical barrier to the surface flow, such as vegetation patches, woody debris or litter; and by the microtopography, such as flat areas or depressions functioning as water-ponding and sediment-trapping areas. Furthermore, for any given vegetation cover and topography, the degree of actual connectivity, runoff source areas effectively connected by runoff flows, would also depend on some key hydrologic variables such as initial soil moisture, rainfall duration, and within-storm fluctuations of rainfall intensity [*Cammeraat*, 2002; *Reaney et al.*, 2004; *Puigdefábregas*, 2005].

[6] Several spatial pattern metrics have been applied to measure the number, size, shape and some aspects of the spatial arrangement of patch and interpatch areas through indices such as lacunarity, proximity, and connectance [*Plotnick et al.*, 1993; *Gustafson and Parker*, 1994; *McGarigal et al.*, 2002]. Some of these landscape metrics are commonly used in the field of conservation biology to assess habitat connectivity and fragmentation [*Calabrese and Fagan*, 2004]. However, while animals or plants can potentially move in any direction, the direction of water or soil fluxes depends on topographic gradients. Indeed, because of the acknowledged importance of microtopography on the connectivity of surface water flows [*Dunne et al.*, 1991; *Solé-Benet et al.*, 1997; *Kirkby et al.*, 2002; *Bedford et al.*, 2006], it is always desirable to combine elevation data with vegetation cover maps when measuring hydrologic connectivity. This fact has been considered in some hydrology specific connectivity metrics recently derived that include topographic information, such as the Leakiness Index [*Ludwig et al.*, 2007] and the integral connectivity scale [*Western et al.*, 2001]. The Leakiness Index combines remotely sensed vegetation patchiness data with elevation data to indicate the potential for landscapes to lose soil sediments within a range of minimum and maximum reference leakiness. The integral connectivity scale [*Western et al.*, 2001] uses topographic data and connectivity functions to characterize the connectivity of soil moisture patterns. This latter tool however was not particularly designed to assess runoff source connectivity, and is not sensitive to the grain size of the bare soil spatial pattern when the bare soil area forms a unique cluster, which is a common situation in many semiarid landscapes.

[7] Studies providing empirical support for direct relationships between currently existing patchiness metrics or connectivity indices and the hydrological functioning of ecosystems are rare [*Bautista et al.*, 2007]. Further, the sensitivity of some of these metrics to different connectivity patterns, as well as their potential to indicate the hydrologic behavior of the system, seem to vary between different semiarid landscapes [*Bastin et al.*, 2002; *Boix-Fayos et al.*, 2006], and may depend on the extent of the targeted study area. For example, the Leakiness index is sensitive to the

total number of pixels in a spatial map, reducing its power to detect small changes in potential leakiness for very large maps unless some corrections are applied [*Ludwig et al.*, 2007]. Thus, more research in this field is needed to assess the strengths and weaknesses of different approaches to hydrologically significant connectivity and their applicability for different regions.

[8] In this work, we derived a simple metric, Flowlength, to measure the connectivity of patchy runoff source areas considering both vegetation cover and topography. The Flowlength index is defined as the average length of all the potential runoff pathways in the target area. Thus, a higher value of the index indicates a higher hydrologic connectivity of runoff source areas. We tested the sensitivity of this connectivity metric to different spatial patterns of runoff sources and runoff sinks, along with its relationships with runoff and sediment yields at the hillslope and catchment scales, in a semiarid grassland-shrubland mosaic landscape in southeast Spain.

2. Materials and Methods

2.1. Study Area

[9] This study was conducted in an instrumented catchment, MC12, located on the south facing slopes of El Ventós Experimental Site (38°28′N, 0°37′W), in the province of Alicante, southeastern Spain. El Ventós Experimental Site is used to long-term monitor vegetation, soil, and water dynamics at various scales in a representative semiarid Mediterranean landscape [*Bellot et al.*, 1998; *Chirino et al.*, 2006], providing the opportunity to empirically test the potential and sensitivity of the new connectivity metric proposed in the work reported here. The catchment MC12 is 23.2 ha in extent and ranges in elevation from 540 to 853 m. The site has a semiarid Mediterranean climate with a long-term average rainfall of 270 mm a^{-1}, which falls mainly in autumn and spring, and an average annual temperature of 18°C. High rainfall variability between and within years is very common in the area. The geology is dominated by limestones of the upper Cretaceous (Cenomanian), which comprise the Ventós-Castellar aquifer. Marls are also present at lower elevations. Soils are generally shallow, thinner than 15 cm on average [*Ramírez*, 2006] and loamy to silty loam in texture [*Bautista et al.*, 2007]. The vegetation cover, around 40% throughout the study catchment, occurs in vegetated patches separated by interconnected bare interpatches. The main vegetation patches are single or clumped individuals of the tussock grass *Stipa tenacissima* L., shrubs (e.g., *Quercus coccifera* L., *Rhamnus lycioides* L, and *Erica multifora* L.), subshrubs (e.g., *Globularia alypum* L.), and mixed patches of the short perennial grass *Brachypodium retusum* (Pers.) P. Beauv. and chamaephytes (e.g., *Teucrium pseudochamaepitys* L., *Fumana ericoides* L.). The interpatches have a high cover of rock fragments and physical and biological soil crusts dominated by lichens and cyanobacteria.

2.2. Hydrological Measurements

[10] Runoff production was measured at plot (16 m^2) and catchment (3−6 ha) scales, while sediment yield was measured only at the plot scale. The monitoring design is shown in Figure 1.
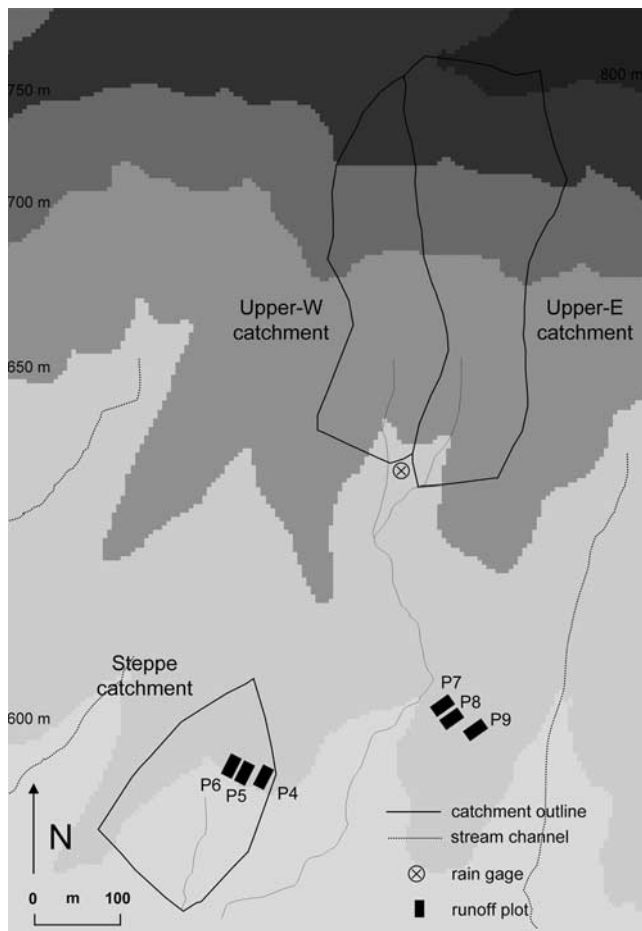
Figure 1. Location of Steppe, Upper-W and Upper-E catchments, and runoff plots within the study area. Vegetation in Steppe catchment and runoff plots P4, P5, and P6 is dominated by the tussock grass *Stipa tenacissima*, while plots P7, P8, and P9 are covered mainly by the short, sod-forming grass *Brachypodium retusum*, subshrubs, and chamaephytes. Vegetation in Upper-W and Upper-E catchments is dominated by *S. tenacissima* and shrub species such as *Quercus coccifera* and *Rhamnus lycioides*.

[11] Six 8 × 2-m closed runoff plots were installed on two different slopes. The plots had similar slope angle (24–26°), aspect (S–SW) and vegetation cover (36–46%), but varied in the density, composition and spatial arrangement of vegetation patches. Total plot runoff and sediment yields were measured after each rainfall event for a period of 45 months. The runoff from each plot was collected in a Gerlach trough connected to a downslope storage tank, where it was measured. Sediments that had settled on the base of the troughs were directly collected, taken to the laboratory, dried (60°C, constant weight) and weighed. The amount of sediments in the runoff was estimated by drying of the runoff samples taken from the collection tanks.

[12] At the catchment scale, runoff discharge was monitored since July 2002 in one 3-ha catchment ("Steppe"), and since April 2003 in two more catchments, Upper-W and Upper-E (3.7 and 6.0 ha in size, respectively). Discharge was continuously measured from V notch weirs in channels equipped with capacitive probes and data loggers that

record water level changes at 30-s intervals. Total runoff and sediments produced on each plot and total runoff produced on each catchment during the respective study periods (March 2002 to December 2005 for the plot scale and July 2002 to December 2006 for the catchment scale) were calculated by summing the event-based data.

[13] Rainfall was measured with two tipping bucket rain gages, one located next to the outlets of Upper-W and Upper-E catchments (Figure 1), with 1-min temporal resolution, and one located about 1.5 km from the experimental plots, as part of a standard meteorological station, which recorded rainfall with a temporal resolution of 5 min. Rainfall was also recorded from two pluviometers located next to the runoff plots. According to the data recorded from the various rain gages, the spatial variation in total rainfall during the study period was negligible.

2.3. Measurement of Connectivity

[14] The connectivity metric derived in this study, Flow-length, is based on the assumption that the majority of bare soil areas behave as sources of runoff and sediments that are trapped by vegetation patches and topographic sinks, such as surface microdepressions, lower on the runoff pathway. This contrasting behavior of bare and vegetated areas has been confirmed by many studies conducted in semiarid Spain [*Cerdà*, 1997; *Puigdefábregas et al.*, 1999; *Bochet et al.*, 2006] and in other semiarid regions worldwide [*Dunkerley and Brown*, 1995; *Reid et al.*, 1999; *Schlesinger et al.*, 1999; *Bhark and Small*, 2003].

[15] Flowlength is obtained from a simple algorithm implemented in a software program designed for this purpose. Pseudocode illustrating this algorithm is included in the auxiliary material.[1] The program calculates the potential length of the runoff path from each cell in a binary map with bare soil pixels classified as runoff sources and vegetation pixels classified as runoff sinks. The flowpaths are defined using a single flow direction (SFD) algorithm [*O'Callaghan and Mark*, 1984], considering the down-gradient direction determined from a digital elevation model (DEM) overlaying the binary map. Unlike the vegetation patches, the topographic sinks are not initially identified in the target map. Instead, the algorithm ends the flowpath when it reaches a pixel with all neighbor pixels being either of higher elevation or already visited by that path. Thus, the path is constrained so that it can only progress downslope from pixel to pixel, along either the cardinal or the diagonal direction, via the neighboring steepest descent pixel, until it reaches a vegetation patch, a surface microdepression, or flows out of the area of interest. In the case of two or more equally steepest descent pixels, the direction of the flowpath is randomly assigned. The effect of this random assignment is expected to be negligible because of the high number of pixels commonly involved in this type of analysis. To test this assumption, we computed Flowlength in repeated runs of the Flowlength program for each of the study plots and catchments, resulting in negligible differences among runs. The results of this sensitivity test are included in the auxiliary material. The length of the flow from a given cell to the next one is computed between the pixels' centers and along the slope, taking into account the between-pixel

---

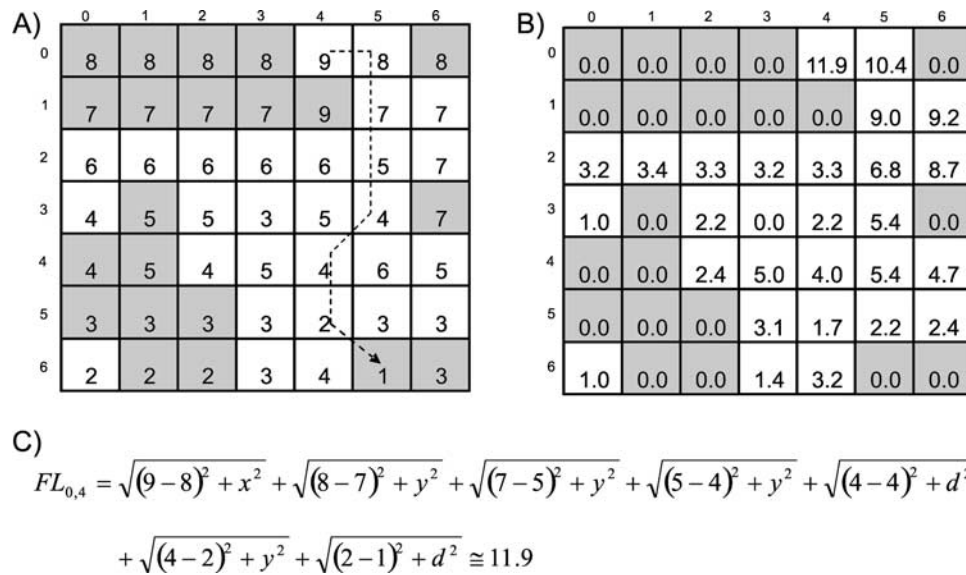[1]Auxiliary materials are available in the HTML. doi:10.1029/2007WR006367.

Figure 2. Graphic representation of the calculations to obtain the Flowlength (FL) index. (a) Vegetation and elevation map of a hillslope. The shaded cells represent vegetation pixels and the white cells represent bare soil pixels. The numeric values represent the pixel elevation. (b) Map of flowpath lengths from each pixel. The value of the FL index (2.5 in this example) is calculated as the average of all flowpath lengths in the map. (c) Calculations to obtain the length of the flowpath indicated by the dashed arrow in Figure 2a. Flowpath length between two successive pixels in a given path is calculated as the length of the slope defined by the difference in elevation between the two pixels and the horizontal distance between them. The píxel size considered in the maps is 1×1 units, hence the horizontal distance between two neighbor pixels along the two cardinal directions are $x = 1$ and $y = 1$, and along the diagonal is $d = \sqrt{2}$. $FL_{0,4}$ = flowpath length for pixel in row 0 and column 4.

difference in altitude and hence yielding values that increase with the slope angle. The selection of a single flow direction (SFD) algorithm to be used in Flowlength calculations was based on the trade-off between simplicity and accuracy. SFD algorithms are commonly used and simple to implement, work well on convergent flows (avoiding dispersion), have a simple and efficient grid-based matrix storage structure, and are robust, coping well with difficult and ambiguous elevation combinations that may arise in real data [*Tarboton*, 1997]. The potential disadvantages of the SFD algorithms as compared with multiple flow direction (MDF) algorithms (e.g., D-infinity) [*Tarboton*, 1997] arise from the discrete assignment of flow into only one of eight possible directions separated by 45° [*O'Callaghan and Mark*, 1984], which may resolve flow direction too coarsely and lead to errors that tend to propagate downslope [*Fairfield and Leymarie*, 1991]. However, since Flowlength is calculated as the average of a large number of flowpaths, many of them being very short, the effects of these potential biases are minimized. Furthermore, the use of high-resolution topographic data could greatly reduce the differences between SFD and MFD algorithms. An example of the calculation of the Flowlength index from a map of vegetation and topography is given in Figure 2. Flowlength index is eventually calculated as the mean of the flowpath lengths of all the cells in the map. Thus, a higher value of Flowlength indicates a higher average length of the runoff pathways and therefore a higher hydrologic connectivity. The potential of Flowlength as an explanatory variable for runoff and sediment yields was tested for total accumulated yields and for the runoff and

sediments produced by a wide range of rainfall size classes. Other statistics describing the frequency distribution of flowpath lengths, such as the average length of the largest flowpaths, were calculated and explored as alternative connectivity indices.

2.4. Vegetation and Topography Maps

[16] At the plot scale, we derived binary source-sink maps from digitalized vegetation maps available for each plot from a previous work [*Bautista et al.*, 2007]. We labeled the bare soil pixels and the vegetation pixels as runoff sources and runoff sinks, respectively. The spatial resolution of these maps is 8 cm, which was considered to be the minimum width for an effective surface obstruction to runoff. The microrelief data were obtained by measuring the distance between the terrain surface and the horizontal plane defined by a leveled frame located over the plot. These measurements were taken on a 10 cm × 10 cm grid, using a graduated ruler with a maximum accuracy of 1 mm. The XYZ coordinates obtained with this field survey were read by the GIS system ESRI®ArcGIS 9.0 (Environmental System Research Institute Inc., California), and a digital elevation model (DEM) with 8-cm pixel size was built for each plot. In addition to the individual actual DEMs, we also generated a common baseline DEM with no rugosity, simulating an idealized planar hillslope, which was applied to each plot in order to study separately the contribution of the microtopography and the contribution of the vegetation pattern to Flowlength values. The baseline DEM, with same size and pixel resolution than the actual DEMs, had equal altitude values for all pixels in the same row, with altitudes
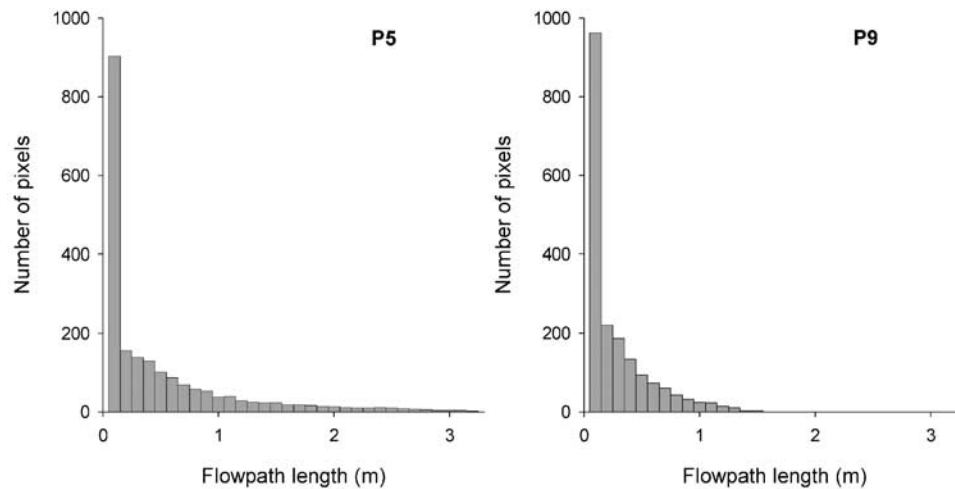
Figure 3. Distribution of flowpath lengths for study plots P5 and P9.

descending from the top to the base of the map so that the slope of the idealized planar hillslope created was equal to the average slope of the runoff plots (25°).

[17] At the catchment scale, the vegetation maps were obtained from a high-resolution (80-cm pixel size) aerial photograph taken in July 1998. This spatial resolution is comparable to the scale of water and sediment redistribution processes in these environments [*Puigdefábregas and Sánchez*, 1996; *Bergkamp et al.*, 1999]. We processed this image and derived classified maps with bare soil pixels labeled as sources and vegetation pixels labeled as sinks of runoff for the three study subcatchments. Rock outcrops are common in the study area, especially in the catchments located in the headwaters, Upper-W and Upper-E, where large and extensively fractured limestone outcrops cover around 20% of the catchment area. The small rock outcrops, generally compact and uniform, are considered to have a low-infiltration capacity and hence to act as runoff sources. However, the large surfaces of fractured limestone outcrops (>3 m length) are considered to be areas of preferential infiltration, on the basis of the fast response of the Ventós-Castellar aquifer after relevant storm events [*Andreu et al.*, 2001]. Nevertheless, this hypothesis remained untested. Thus, we built and tested two different maps for each catchment: (1) considering the large rock outcrops as runoff sinks and (2) considering them as runoff sources. The topographic information for the study catchments was obtained from an available DEM of El Ventós Experimental Site at 5-m spatial resolution, built from a 1:10000 topographic map. This DEM was resampled to match the 0.8-m grid-based vegetation data.

3. Results

3.1. Connectivity of Runoff Source Areas

[18] The distribution of individual flowpath lengths for all the plots and catchments analyzed was strongly skewed to the right. Figure 3 shows two contrasting examples of flowpath length distribution from runoff plots. The large number of zero values corresponds mostly with vegetation pixels, yet some zero values may also correspond with pixels inside a microdepression. Since total plant cover values on the study plots were very similar (36–46%), the number of zero values varied only slightly between plots. However, the distribution of flowpaths larger than zero ranged from relatively wide distributions including several classes of long flowpaths (e.g., P5, Figure 3) to narrow distributions highly dominated by short and very short flowpaths (e.g., P9, Figure 3).

[19] The metric Flowlength classified the runoff plots along a continuum from low to high connectivity of bare soil (Figure 4). The connectivity increased with the grain size of the bare soil spatial pattern, which was higher in the plots where the vegetation cover was distributed in a lower number of bigger patches (Figure 4). In agreement with the differences in the spatial resolution used, Flowlength values for the study catchments were higher than from the study plots (Figures 5, 6, and 7). Flowlength was much higher when the large rock outcrops were considered as runoff sources.

[20] When the idealized planar slopes were considered in the calculation of the flowpath lengths, the Flowlength values were higher (p = 0.045; d.f. = 8; Paired sampled T-test) than those obtained with the real microtopography (Figures 4, 5, 6, and 7). At the catchment scale, these differences were particularly marked when the rock outcrops were considered as runoff sources (Figures 5, 6, and 7). The microtopography of the runoff plots was characterized by structures generally associated with the vegetation patches. Most plant patches, particularly, *Stipa tenacissima* tussocks and big shrubs, formed terracettes with nearly flat areas of deposited sediments on the upslope side of the plants.

3.2. Rainfall, Runoff, and Erosion

[21] The first 3 years of the study period (2002–2004), annual rainfall (241, 256 and 275 mm, respectively) was close to the long-term average (270 mm). That period was followed by a dry year (183 mm), which was followed by a relatively wet year (352 mm). The maximum rainfall amount and 15-min rainfall intensity recorded during the study period were 46 mm and 51 mm h^{-1}, respectively, which corresponded to an event of 4 years of return period. The majority of rainfall events were of low magnitude: 79% of the events were less than 5 mm, 89% of the events were
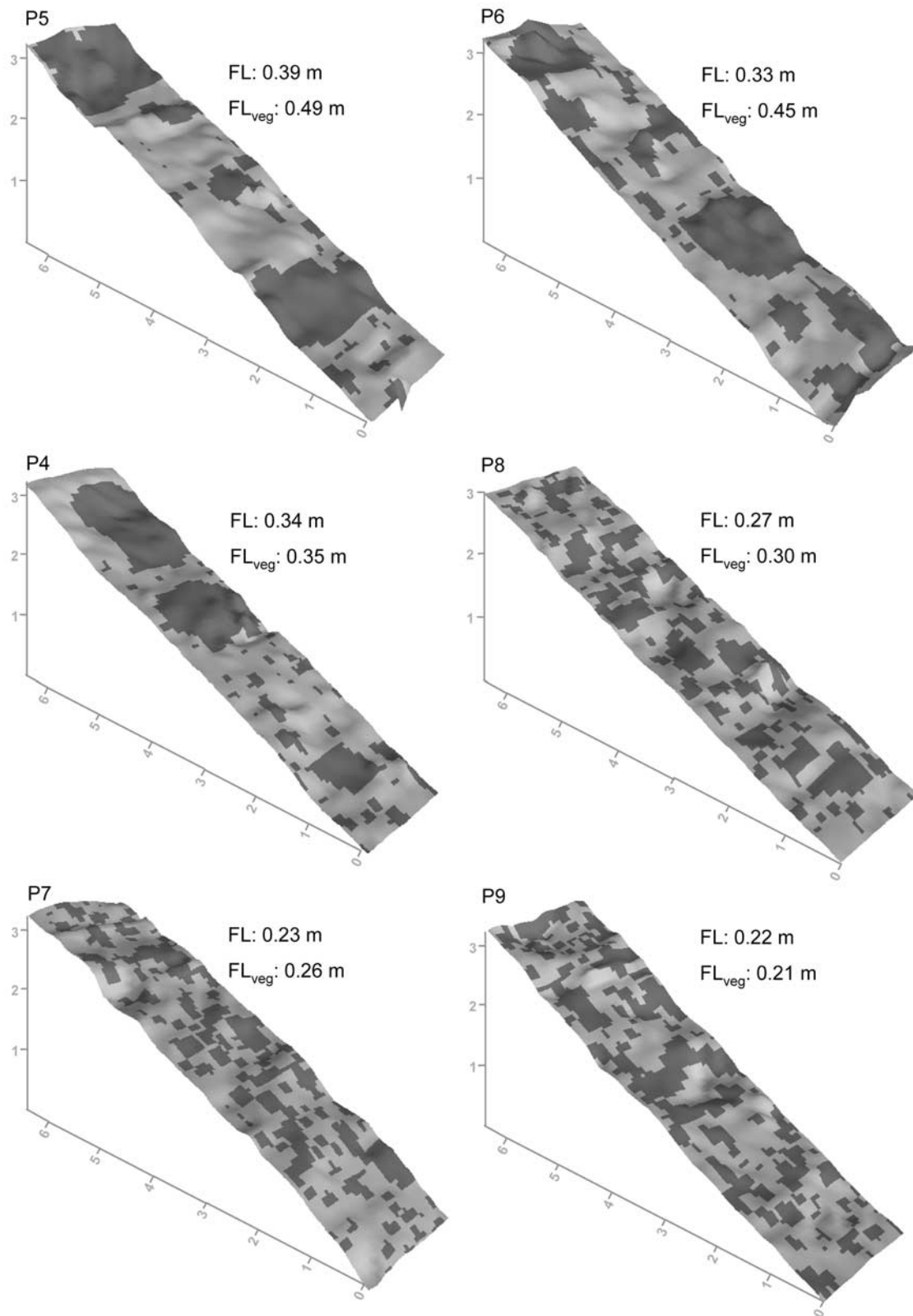
Figure 4. Maps of vegetation and microtopography of the experimental plots. The dark grey patches correspond to vegetation, and the light grey interpatches correspond to bare soil. The plots are arranged from higher to lower connectivity of bare soil, from top to bottom and from left to right, according to Flowlength (FL) values. FL_{veg} corresponds to Flowlength values obtained from the vegetation maps, without considering the microtopography.
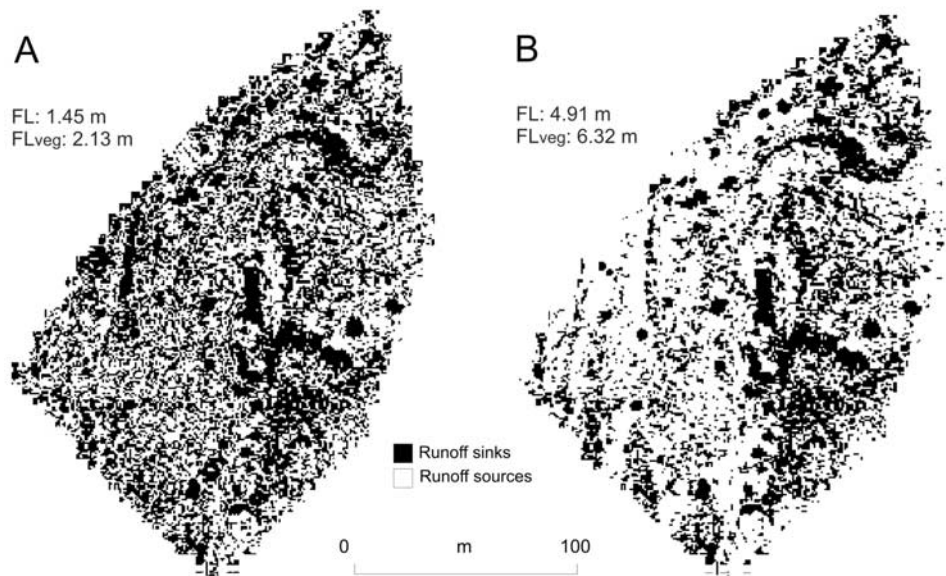
Figure 5. Maps of runoff sources and runoff sinks of the Steppe catchment, considering as runoff sinks (a) the vegetation and large rock outcrops or (b) the vegetation alone. Flowlength values are shown for each map. FL_{veg} corresponds to Flowlength values obtained from the vegetation maps, without considering the microtopography.

less than 10 mm, and only 2% of the events exceeded 30 mm.

[22] At the plot scale, runoff events were relatively frequent (around 14 events per year, while sediment events were much more scarce (around 5 events per year). Both runoff and sediments produced by individual rainfall events showed a highly skewed distribution, with 50% of the total runoff and sediments yielded by 6 and 2 storms, respectively (Figure 8). Runoff and sediment yield were also highly variable between plots [*Bautista et al.*, 2007]. Total runoff produced on the study plots ranged from 3.7 mm (plot P9) to 18.9 mm (plot P5), and sediment yield ranged from 4.7 g m^{-2} (plot P9) to 19.8 g m^{-2} (plot P5). At the catchment scale, runoff events were infrequent. During the measuring period at this scale (53 months), the study catchments produced runoff only on four occasions. Total catchment runoff for this period is shown in Figure 9. The Upper-W and Upper-E catchments yielded similar total amounts of runoff ($\approx$0.24 mm), while the Steppe catchment produced more than twice this value.

3.3. Relationships Between Connectivity and Runoff

[23] The connectivity metric, Flowlength, was linearly and positively related to both total plot runoff and sediment yields (Figure 10). These relationships were better for the values of Flowlength obtained from actual elevation data than for the values obtained from the planar slopes (Figure 10). We compared Flowlength (average of all flowpath lengths in the map) with the average length of different flowpath length classes as explanatory variables for total runoff and sediment yields. The variation in total plot runoff and sediment yields explained by Flowlength was similar to the variation explained by the average of the 5%, 10%, 20%, 25%, 30%, 40%, and 50% largest values of flowpath lengths, and higher than the variation explained by the average length of the 1% longest flowpaths (Figure 11).

[24] The role of rainstorm size in the relationship between Flowlength and runoff is shown in Figure 12. The strongest relationships were observed for the accumulated runoff produced by moderate- and high-magnitude rainfall events (>20 mm). The variation in runoff explained by Flowlength decreased for low-magnitude rainfalls, being insignificant for the smallest rainfall events (<5 mm) (Figure 12). Because of the relatively low number of sediment events
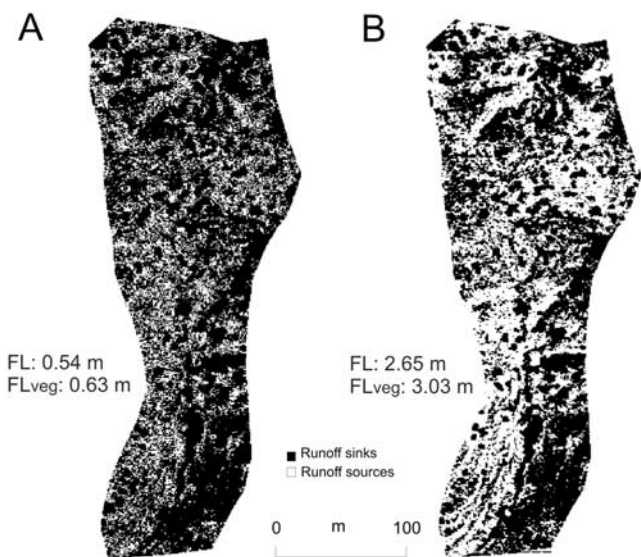

Figure 6. Maps of runoff sources and runoff sinks of the Upper-E catchment, considering as runoff sinks (a) the vegetation and large rock outcrops or (b) the vegetation alone. Flowlength values are shown for each map. FL_{veg} corresponds to Flowlength values obtained from the vegetation maps, without considering the microtopography.
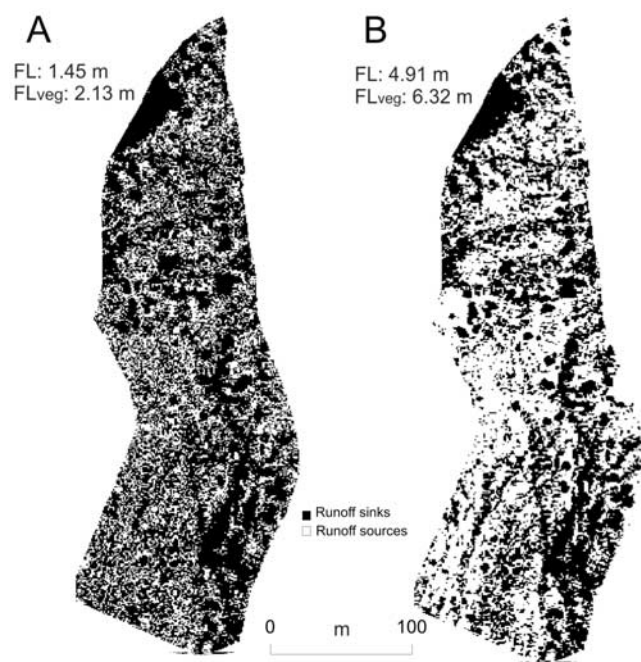
Figure 7. Maps of runoff sources and runoff sinks of the Upper-W catchment, considering as runoff sinks (a) the vegetation and large rock outcrops or (b) the vegetation alone. Flowlength values are shown for each map. FL_{veg} corresponds to Flowlength values obtained from the vegetation maps, without considering the microtopography.

produced during the study period, only three rainstorm size intervals (>20 mm, 10–20 and <10 mm) were considered in the analysis of the Flowlength explanatory potential for sediment yield. The covariation between sediment yield and Flowlength was only significant for the highest-magnitude rainfall events (>20 mm), with the coefficient of determination, R^2, ranging from 0.709 (for rainstorms > 20 mm) to 0.576 (for rainstorms of 10–20 mm).

[25] The three study catchments were equally ranked according to total catchment runoff produced during the study period and Flowlength values, either considering the large rock outcrops as runoff sinks or as runoff sources (Figure 9). However, the between-catchment differences in the magnitude of total runoff better matched the Flowlength

variation when the large rock outcrops were considered as runoff sinks.

4. Discussion

[26] The connectivity metric derived in this work, Flowlength, is sensitive to the spatial configuration of runoff sink and runoff source areas in the landscape. Thus, Flowlength values from our study plots increased with the grain size of the spatial pattern of the bare soil areas. Flowlength combines the spatial configuration of the vegetation cover with the topography (which determines the direction of the surface flow and its interruption in the case of depressions), thereby improving the assessment of potential water flow connectivity in comparison to other spatial pattern metrics that are solely based on plant cover data [e.g., *McGarigal et al.*, 2002], particularly in the case of topographically complex terrains such as many arid and semiarid landscapes. In addition, Flowlength values increase with slope angle, which both increases the velocity of runoff along the flowpaths and decreases the opportunity for run-on infiltration, thus increasing runoff magnitude [*Wainwright and Parsons*, 2002]; both processes entail an increase in the kinetic energy of the flow and thus a potential increase in flowpath length.

[27] Flowlength quantifies the length of all the potential runoff flowpaths in the area of interest, whether the bare soil forms isolated patches or a single continuous cluster – thus Flowlength can be applied to a wider range of patterns and conditions relative to other indices that also consider the topography, such as the integral connectivity scale [*Western et al.*, 2001]. Flowlength quantifies the potential connectivity of bare soil areas for any spatial extent, without considering baseline or reference conditions. However, the ecological and hydrological implications of the connectivity assessed may vary among landscapes, depending on the interactions with other factors such as soil type, climatic conditions, and ecosystem type.

[28] Vegetation cover is considered a good explanatory variable for runoff and sediment yields [e.g., *Elwell and Stocking*, 1976; *Thornes*, 1990]. However, recent studies have shown that vegetation pattern also plays an important role in the functioning of semiarid ecosystems [e.g., *Bautista et al.*, 2007; *Kéfi et al.*, 2007], and that landscape metrics derived from plant spatial patterns are good indicators of the
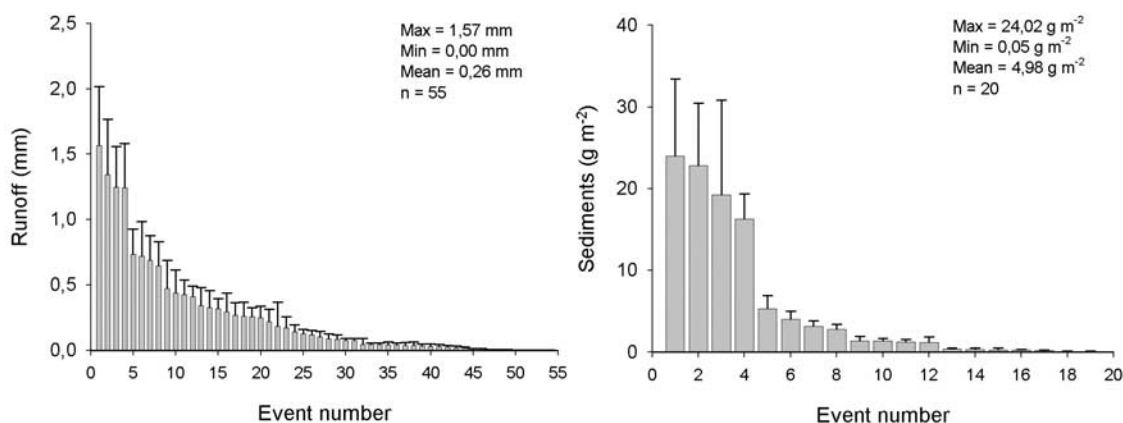

Figure 8. Event runoff and sediment yield (mean values and standard errors) produced by the six experimental plots over the 45-months study period. Events are ranked by magnitude.
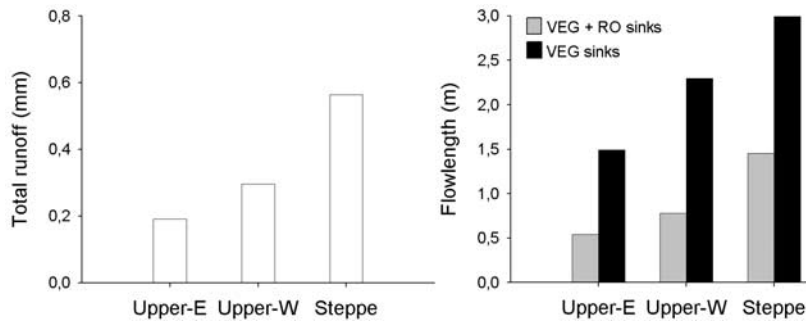
Figure 9. Total runoff and Flowlength for the three study catchments. Flowlength values were obtained considering only the vegetation patches (VEG) as runoff sinks or both the vegetation patches and large rock outcrops (RO) as runoff sinks.

hydrological behavior of semiarid landscapes [*Bautista et al.*, 2007]. Flowlength was designed to vary with both vegetation spatial pattern and vegetation cover, and thereby better explain the hydrological response of semiarid landscapes in comparison to other simple metrics such as vegetation cover, patch density, patch size, etc.

[29] Of several potential descriptors of the frequency distribution of the flowpath lengths, we selected the mean length of all the flowpaths in the target area to be the Flowlength index. We wanted the index to be sensitive to both the largest values, which were expected to be crucial for the hydrological response, and also to the zero values, which correspond mainly to vegetation pixels. Thus, although the frequency distributions of flowpath lengths are highly skewed to the right, differences in connectivity derived from plant cover variation and large flowpaths could be better captured by the average length of all the flowpaths than by other robust statistics of central tendency. The results showed that total runoff and sediment yields were similarly explained by the average length of all the flowpaths than by the average length of the medium to long flowpaths. These results highlight the important role of the longest flowpaths in controlling hillslope water flows. It is likely that runoff and sediment yields are even more closely related to the longest flowpaths when concentrated overland flow is the main process driving the hydrology of the target area.

[30] The observed relationships between Flowlength and total plot runoff and sediment yields are some of the first empirical demonstrations of the role of the connectivity of bare soil areas in the hydrological response of semiarid hillslopes. Our results show that a coarsening of the spatial pattern of runoff source areas leads to an associated increase in their hydrological connectivity (P5 to P9 in Figure 4), which should increase flow concentration, velocity, and thus erosive power. These results support the hypotheses established by a number of studies and conceptual models from semiarid regions worldwide [*Abrahams et al.*, 1995; *Tongway and Ludwig*, 1997; *Davenport et al.*, 1998; *Schlesinger et al.*, 1999; *Wainwright et al.*, 2000; *Bartley et al.*, 2006]. Our results also are in agreement with recent simulation-modeling works predicting that clumped vegetation patterns yield more runoff and sediments than spatially uniform distributions, particularly in the case of coarsely aggregated vegetation patterns [*Boer and Puigdefábregas*, 2005].
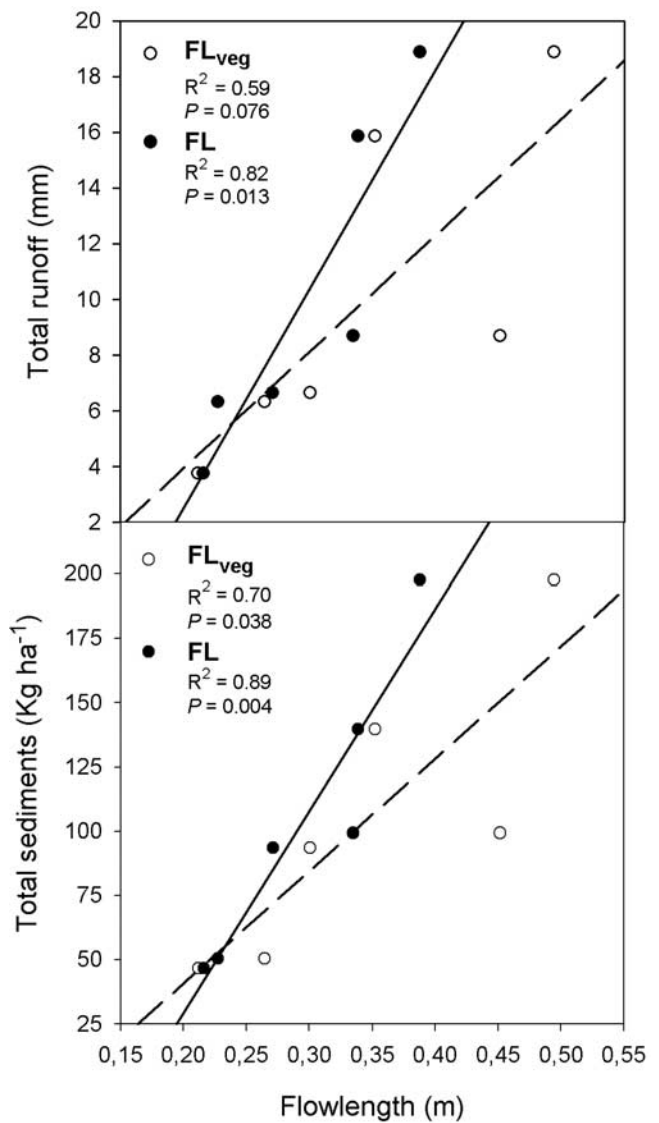

Figure 10. Total runoff and total sediment yield in the six experimental plots versus Flowlength. Flowlength values were calculated considering both the vegetation pattern and the microtopography (FL) and only considering the vegetation pattern (FLveg).
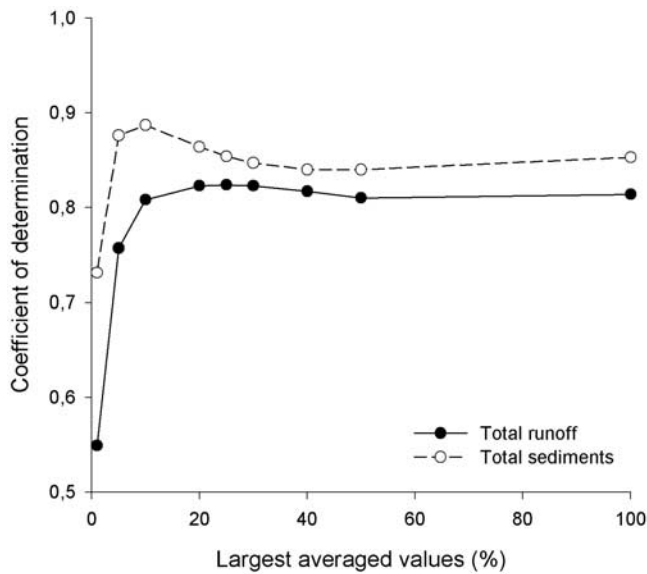
Figure 11. Coefficients of determination (N = 6) of the linear regression between total runoff or total sediment yields in the experimental plots and the average of the 1%, 5%, 10%, 20%, 25%, 30%, 40%, 50%, and 100% largest values of flowpath lengths.

[31] The strength of the correlation between Flowlength and runoff and sediment yields increases with the storm size, being less clear for small events. In semiarid lands, runoff and sediment events typically show skewed distributions [e.g., *Wilcox et al.*, 2003], with few large events producing the majority of the total runoff and sediments. Therefore, since Flowlength is a good explanatory variable for runoff and sediments yielded by the most productive rainfall events, it is expected to accurately assess the potential for runoff and sediment production of semiarid ecosystems. The decrease in the strength of the relationships between the connectivity of bare soil areas and runoff and sediment yields for low-magnitude rainfall events, suggests that most source areas are only effectively connected by runoff during high- to moderate-magnitude storms. These results are in agreement with previous studies [*Bergkamp*, 1998; *Calvo-Cases et al.*, 2003; *Bautista et al.*, 2007] reporting that plot runoff and sediments produced by small rainfall events are mostly generated from bare areas close to the collecting trough.

[32] The few runoff events produced at the catchment scale as compared with plot-scale runoff yields shows that, as in many other semiarid landscapes [*Wilcox et al.*, 2003], unit area runoff decreases as scale increases in our study site. The influence of the connectivity of the runoff source areas on runoff production was also supported by the catchment-scale data. The results at this scale are not conclusive about the role of the rock outcrops as runoff source or runoff sink areas. However, the evidence provided by between-catchment comparisons of Flowlength and total runoff values suggests that the large, highly fractured outcrops primarily function as runoff sink areas. This is in agreement with our field observations of surface runoff

patterns during or after rainfall, and with the rapid recharge response of the aquifer underneath the study area to rainfall events [*Andreu et al.*, 2001].

[33] For theoretical uniform-gradient hillslopes, runoff sink areas are primarily the surface obstructions created by vegetation patches and related woody debris and litter. However, in real morphologically varied landscapes, diminished connectivity can also be produced by topographic runoff sinks, such as flat areas or microdepressions functioning as sediment-trapping and water-ponding areas. Conversely, microtopographic patterns can increase hillslope connectivity by causing the convergence of runoff flowpaths into preferential channels and rills. In our study plots, rills were not observed, and the storage capacity of microdepressions was low because of the strong slope gradient [*Kirkby et al.*, 2002]. However, we did observe microtopographic effects on bare soil connectivity due to the flat terracettes that typically occur immediately upslope of vegetation patches.

[34] At El Ventós site, the terracettes associated with vegetation patches result in a net increase in the amount and extent of runoff sink areas, thereby decreasing hillslope connectivity in comparison to the effects of the vegetation patches alone. The effect of soil mounds and terracettes on the convergence or divergence of the flow and bare soil connectivity depends on their shape and size, the overall slope gradient, and the type of storm, among other factors [*Boer and Puigdefábregas*, 2005]. For a given vegetation type, terracettes developed upslope of the vegetation patches are common on moderate to steep slopes, where
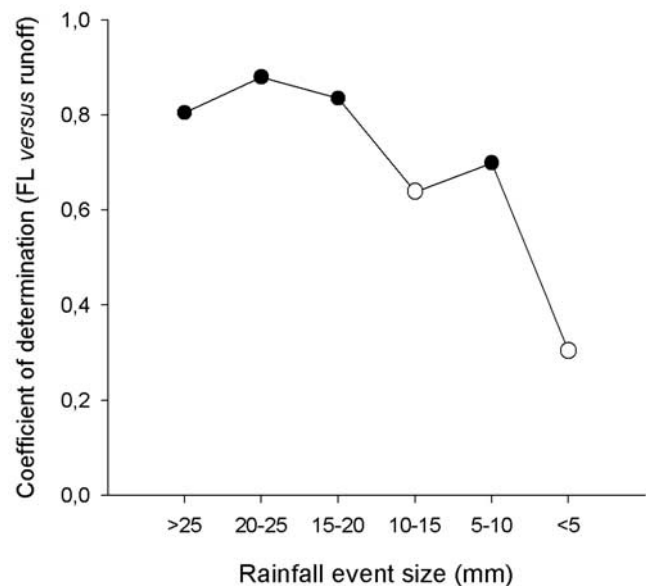

Figure 12. Coefficients of determination (N = 6) of the linear regression between Flowlength and the accumulated runoff in the experimental plots produced by rainfall events of different size: >25 mm (N = 11), 20–25 mm (N = 3), 15–20 mm (N = 7), 10–15 mm (N = 11), 5–10 mm (N = 14), and <5 mm (N = 6). Black and white circles indicate significant (P < 0.05) and nonsignificant (P > 0.05) relationships, respectively.

runoff is the main agent of sediment transport and deposition [*Sánchez and Puigdefábregas*, 1994; *Cammeraat and Imeson*, 1999; *Bochet et al.*, 2000]. In contrast, mound-type structures are dominant on gentle slopes where differential interrill and splash erosion beneath and outside plant cover, and trapping of wind-transported sediment and organic debris are the main processes driving mound development [*Parsons et al.*, 1992; *De Soyza et al.*, 1997; *Bochet et al.*, 2000]. On gentle slopes dominated by mound-type structures, where more or less symmetric mounds develop under the plants, or in areas where interpatch channels are important, the vegetation patches are confined to the highest parts of the microtopography [*Dunne et al.*, 1991; *Solé-Benet et al.*, 1997; *Bedford et al.*, 2006] and are less able to disconnect the flow. In these situations, the contribution of the microtopography is expected to increase the measured connectivity of runoff sources.

[35] The inclusion of microtopographic information in the quantification of runoff source connectivity significantly improved the relationships between the connectivity metric and the measured flows at the plot scale. At the catchment scale, the contribution of microtopography to the relationships between Flowlength and runoff could not be properly tested because of the small number of cases and the low pixel resolution of the raw elevation data (5 m). However, it is worth noticing that all three catchments analyzed showed a consistent decreasing effect of microtopography on Flowlength when rock outcrops were considered as runoff sources, which may be explained by the discontinuity in the runoff source flowpaths due to protruding outcrops.

[36] Flowlength is derived from raster-based maps obtained from either field survey mapping or aerial photography and high-resolution satellite images, and thus can be applied to assess connectivity at various spatial extents. Obviously the sensitivity of Flowlength is expected to depend on the quality (resolution and accuracy) of the vegetation and topographic data, which may also depend on the scale of the assessment. Thus, with more precisely resolved topographic data (improved vertical and/or horizontal resolution), runoff flowpaths and the associated degree of connectivity can be more accurately defined, particularly when using SFD algorithms [*Pan et al.*, 2004]. Ideally, DEM resolution should match the vegetation map resolution. However, the relative importance of the topographic data resolution and accuracy depends on the role of the microrelief in determining water flows in any particular landscape. For example, in our study area, for the whole set of plot vegetation maps analyzed, the Flowlength values obtained from high-resolution DEMs were only slightly different than the Flowlength values obtained with the low-resolution baseline DEM with no rugosity (Figure 4). These results point out that the connectivity of runoff sources at our study site is mainly controlled by the spatial distribution of vegetation patches.

[37] Our results show that the Flowlength index has potential for improving assessments of the hydrological functioning of patchy semiarid ecosystems. In arid and semiarid areas affected by land degradation, this functioning is progressively lost (see several examples given by *Ludwig et al.* [2005]). The Flowlength index could be very useful for both analyzing the consequences of land degradation in landscape connectivity and thereby in the hydrologic functioning, and prioritizing areas for rehabilitation and restoration to mitigate degradation processes.

5. Conclusions

[38] The index of connectivity developed in this study, Flowlength, quantifies the connectivity of runoff source areas using vegetation and topography data. This metric is sensitive to plant cover and spatial pattern, surface rugosity, and slope angle, which are key determinants of hillslope and catchment hydrology, particularly in drylands. We found strong positive relationships between Flowlength and hillslope runoff and sediment yields. In our study area, the connectivity of runoff source areas is mainly controlled by the vegetation pattern, with Flowlength values increasing with the grain size of the bare soil pattern. However, the Flowlength index here also reflects microtopographic roughness and sinks created by mounds and terracettes associated with the plant patches, which also affects hillslope runoff and sediment yields. Although some uncertainty remains at the catchment scale, and the applicability of the Flowlength metric to other regions and landscape patterns requires further testing, our results demonstrate its potential for assessing hillslope and catchment conditions relative to potential runoff and sediment losses in semiarid lands.

References

Abrahams, A., A. J. Parsons, and J. Wainwright (1995), Effects of vegetation change on interrill runoff and erosion, Walnut Gulch, southern Arizona, *Geomorphology*, 13, 37–48, doi:10.1016/0169-555X(95)00027-3.

Aguiar, M. R., and O. E. Sala (1999), Patch structure, dynamics and implications for the functioning of arid ecosystems, *Trends Ecol. Evol.*, 14, 273–277, doi:10.1016/S01695347(99)01612-2.

Andreu, J. M., J. Delgado, E. García-Sánchez, A. Pulido-Bosch, J. Bellot, E. Chirino, and J. M. Ortíz De Urbina (2001), Caracterización del funcionamiento y la recarga del acuífero Ventós-Castellar (Alicante), *Rev. Soc. Geol. Esp.*, 14, 247–254.

Bartley, R., C. H. Roth, J. Ludwig, D. McJannet, A. Liedloff, J. Corfield, A. Hawdon, and B. Abbott (2006), Runoff and erosion from Australia's tropical semi-arid rangelands: Influence of ground cover for differing space and time scales, *Hydrol. Processes*, 20, 3317–3333, doi:10.1002/hyp.6334.

Bastin, G. N., J. A. Ludwig, R. W. Eager, H. Chewings, and C. Liedloff (2002), Indicators of landscape function: Comparing patchiness metrics using remotely sensed data from rangelands, *Ecol. Indicators*, 1, 247–260, doi:10.1016/S1470-160X(02)00009-2.

Bautista, S., A. G. Mayor, J. Bourakhouadar, and J. Bellot (2007), Plant spatial pattern predicts hillslope runoff and erosion in a semiarid Mediterranean landscape, *Ecosystems*, 10, 987–998, doi:10.1007/s10021-007-9074-3.

Bedford, D. R., E. E. Small, G. E. Tucker, and W. T. Pockman (2006), Effect of soil and vegetation heterogeneity on runoff in a semi-arid grassland, *Eos Trans. AGU*, 87(52), Fall Meet. Suppl., Abstract H33H–07.

Bellot, J., J. R. Sánchez, A. Bonet, E. Chirino, F. Abdelli, N. Hernández, and J. M. Martínez (1998), Effect of different vegetation type cover on the soil water balance in semi-arid areas of south eastern Spain, *Phys. Chem. Earth*, 24, 353–357.

Bergkamp, G. (1998), A hierarchical view of the interactions of runoff and infiltration with vegetation and microtopography in semiarid shrublands, *Catena*, 33, 201–220, doi:10.1016/S0341-8162(98)00092-7.

Bergkamp, G., A. Cerdà, and A. C. Imeson (1999), Magnitude-frequency analysis of water redistribution along a climate gradient in Spain, *Catena*, 37, 129–146, doi:10.1016/S0341-8162(98)00058-7.

Bhark, E. W., and E. E. Small (2003), Association between plant canopies and the spatial patterns of infiltration in shrubland and grassland of the Chihuahuan desert, New Mexico, *Ecosystems*, 6, 185–196, doi:10.1007/s10021-002-0210-9.

Bochet, E., J. Poesen, and J. L. Rubio (2000), Mound development as an interaction of individual plants with soil, water erosion and sedimentation processes on slopes, *Earth Surf. Processes Landforms*, 25, 847–867, doi:10.1002/1096-9837(200008)25:8<847::AID-ESP103>3.0.CO;2-Q.

Bochet, E., J. Poesen, and J. L. Rubio (2006), Runoff and soil loss under individual plants of a semiarid Mediterranean shrubland: Influence of plant morphology and rainfall intensity, *Earth Surf. Processes Landforms*, 31, 536–549, doi:10.1002/esp.1351.

Boer, M., and J. Puigdefábregas (2005), Effects of spatially structured vegetation patterns on hillslope erosion in a semiarid Mediterranean environment: A simulation study, *Earth Surf. Processes Landforms*, 30, 149–167, doi:10.1002/esp.1180.

Boix-Fayos, C., M. Martínez-Mena, E. Arnau-Rosalén, A. Calvo-Cases, V. Castillo, and J. Albaladejo (2006), Measuring soil erosion by field plots: Understanding the sources of variation, *Earth Sci. Rev.*, 78, 257–285.

Calabrese, J. M., and W. F. Fagan (2004), A comparison-shopper's guide to connectivity metrics, *Front. Ecol. Environ*, 2, 529–536.

Calvo-Cases, A., C. Boix-Fayos, and A. C. Imeson (2003), Runoff generation, sediment movement and soil water behaviour on calcareous (limestone) slopes of some Mediterranean environments in southeast Spain, *Geomorphology*, 50, 269–291.

Cammeraat, L. H. (2002), A review of two strongly contrasting geomorphological systems within the context of scale, *Earth Surf. Processes Landforms*, 27, 1201–1222, doi:10.1002/esp.421.

Cammeraat, L. H., and A. C. Imeson (1999), The evolution and significance of soil-vegetation patterns following land abandonment and fire in Spain, *Catena*, 37, 107–127, doi:10.1016/S0341-8162(98)00072-1.

Cerdà, A. (1997), The effect of patchy distribution of *Stipa tenacissima* L. on runoff and erosion, *J. Arid Environ.*, 9, 27–38.

Chirino, E., A. Bonet, J. Bellot, and J. R. Sánchez (2006), Effects of 30-year-old Aleppo pine plantations on runoff, soil erosion, and plant diversity in a semi-arid landscape in south eastern Spain, *Catena*, 65, 19–29, doi:10.1016/j.catena.2005.09.003.

Davenport, D. W., D. D. Breshears, B. P. Wilcox, and C. D. Allen (1998), Viewpoint: Sustainability of piñon-juniper ecosystems: A unifying perspective of soil erosion thresholds, *J. Range Manage.*, 51, 231–240, doi:10.2307/4003212.

De Soyza, A. G., W. G. Whitford, E. Martinez-Meza, and J. W. Van Zee (1997), Variation in creosotebush (*Larrea tridentata*) canopy morphology in relation to habitat, soil fertility and associated annual plant communities, *Am. Midl. Nat.*, 137(1), 13–26, doi:10.2307/2426751.

Dunkerley, D. L., and K. J. Brown (1995), Runoff and runon areas in a patterned chenopod shrubland, arid western New South Wales, Australia: Characteristics and origin, *J. Arid Environ.*, 30, 41–55, doi:10.1016/S0140-1963(95)80037-9.

Dunne, T., W. Zhang, and B. F. Aubry (1991), Effects of rainfall, vegetation and microtopography on infiltration and runoff, *Water Resour. Res.*, 27, 2271–2285, doi:10.1029/91WR01585.

Elwell, H. A., and M. A. Stocking (1976), Vegetal cover to estimate soil erosion hazard in Rhodesia, *Geoderma*, 15, 61–70, doi:10.1016/0016-7061(76)90071-9.

Fairfield, J., and P. Leymarie (1991), Drainage networks from grid digital elevation models, *Water Resour. Res.*, 27(5), 709–717, doi:10.1029/90WR02658.

Gardner, R. H., M. G. Turner, V. H. Dale, and R. V. O'Neill (1992), A percolation model of ecological flows, in *Landscape Boundaries: Consequences for Biotic Diversity and Ecological Flows*, *Ecol. Stud.*, vol. 92, pp. 259–260, Springer, New York.

Gustafson, E. J., and G. R. Parker (1994), Using an index of habitat patch proximity for landscape design, *Landscape Urban Plann.*, 29, 117–130, doi:10.1016/0169-2046(94)90022-1.

Kéfi, S., M. Rietkerk, C. L. Alados, Y. Pueyo, V. P. Papanastasis, A. ElAich, and P. C. de Ruiter (2007), Spatial vegetation patterns and imminent desertification in Mediterranean arid ecosystems, *Nature*, 449, 213–217, doi:10.1038/nature06111.

Kirkby, M., L. Bracken, and S. Reaney (2002), The influence of land use, soil and topography on the delivery of hillslope runoff to channels in SE

Spain, *Earth Surf. Processes Landforms*, 27, 1459–1473, doi:10.1002/esp.441.

Ludwig, J. A., and D. J. Tongway (1995), Spatial organisation of landscapes and its function in semi-arid woodlands, Australia, *Landscape Ecol.*, 10, 51–63, doi:10.1007/BF00158553.

Ludwig, J. A., B. P. Wilcox, D. D. Breshears, D. J. Tongway, and A. C. Imeson (2005), Vegetation patches and runoff-erosion as interacting ecohydrological processes in semiarid landscapes, *Ecology*, 86, 288–297, doi:10.1890/03-0569.

Ludwig, J. A., G. N. Bastin, V. H. Chewings, R. W. Eager, and A. C. Liedloff (2007), Leakiness: A new index for monitoring the health of arid and semiarid landscapes using remotely sensed vegetation cover and elevation data, *Ecol. Indic.*, 7, 442–454, doi:10.1016/j.ecolind.2006.05.001.

McGarigal, K., S. A. Cushman, M. C. Neel, and E. Ene (2002), FRAGSTATS: Spatial Pattern Analysis Program for Categorical Maps, www.umass.edu/landeco/research/fragstats/fragstats.html, Univ. of Mass., Amherst, 30 April 2007.

Nicolau, J. M., A. Solé-Benet, J. Puigdefábregas, and L. Gutiérrez (1996), Effects of soil and vegetation on runoff along a catena in semi-arid Spain, *Geomorphology*, 14, 297–309, doi:10.1016/0169-555X(95)00043-5.

O'Callaghan, J. F., and D. M. Mark (1984), The extraction of drainage networks from digital elevation data, *Comput. Vision Graphics Image Processes*, 28, 323–344, doi:10.1016/S0734-189X(84)80011-0.

Pan, F., C. D. Peters-Lidard, M. J. Sale, and A. W. King (2004), A comparison of geographical information systems–based algorithms for computing the TOPMODEL topographic index, *Water Resour. Res.*, 40, W06303, doi:10.1029/2004WR003069.

Parsons, A. J., A. D. Abrahams, and J. R. Simanton (1992), Microtopography and soil-surface materials on semi-arid hillslope, southern Arizona, *J. Arid Environ.*, 22, 107–115.

Plotnick, R. E., R. H. Gardner, and R. V. O'Neill (1993), Lacunarity indices as measures of landscape texture, *Landscape Ecol.*, 8, 201–211, doi:10.1007/BF00125351.

Puigdefábregas, J. (2005), The role of vegetation patterns in structuring runoff and sediment fluxes in drylands, *Earth Surf. Processes Landforms*, 30, 133–147, doi:10.1002/esp.1181.

Puigdefábregas, J., and G. Sánchez (1996), Geomorphological implications of vegetation patchiness on semi-arid slopes, in *Advances in Hillslope Processes*, vol. 2, edited by M. Anderson and S. Brooks, pp. 1027–1060, John Wiley, London.

Puigdefábregas, J., A. Solé, L. Gutierrez, G. Barrio, and M. Boer (1999), Scales and processes of water and sediment redistribution in drylands: Results from the Rambla Honda field site in southeast Spain, *Earth Sci. Rev.*, 48, 39–70, doi:10.1016/S0012-8252(99)00046-X.

Ramírez, D. (2006), Estudio de la transpiración del esparto (*Stipa tenacissima* L.) en una cuenca del semiárido alicantino: Un análisis pluriescalar, Ph.D. thesis, Univ. de Alicante, Alicante, Spain.

Reaney, S., M. Kirkby, and L. Bracken (2004), The influence of storm characteristics on runoff generation and connectivity on semi-arid hillslopes, *Geophys. Res. Abstr.*, 6, Abstract 05987.

Reid, K. D., B. Wilcox, D. Breshears, and L. MacDonald (1999), Runoff and erosion in a piñon-juniper woodland: Influence of vegetation patches, *Soil Sci. Soc. Am. J.*, 63, 1869–1879.

Sánchez, G., and J. Puigdefábregas (1994), Interaction between plant growth and sediment movement in semi-arid slopes, *Geomorphology*, 9, 243–260, doi:10.1016/0169-555X(94)90066-3.

Schlesinger, W. H., A. D. Abrahams, A. J. Parsons, and J. Wainwright (1999), Nutrient losses in runoff from grassland and shrubland in southern New Mexico: I. Rainfall simulation experiments, *Biogeochemistry*, 45, 21–34.

Solé-Benet, A., A. Calvo, A. Cerdà, R. Lázaro, R. Pini, and J. Barbero (1997), Influences of micro-relief patterns and plant cover on runoff related processes in badlands from Tabernas (SE Spain), *Catena*, 31, 23–28, doi:10.1016/S0341-8162(97)00032-5.

Stauffer, D. (1985), *Introduction to Percolation Theory*, Taylor and Francis, London.

Tarboton, D. G. (1997), A new method for the determination of flow directions and upslope areas in grid digital elevation models, *Water Resour. Res.*, 33(2), 309–319, doi:10.1029/96WR03137.

Thornes, J. B. (Ed.) (1990), *Vegetation and Erosion: Processes and Environments*, John Wiley, Chichester, U. K.

Tongway, D. J., and J. A. Ludwig (1997), The conservation of water and nutrients within landscapes, in *Landscape Ecology Function and Management: Principles From Australia's Rangelands*, edited by J. A. Ludwig et al., pp. 13–22, CSIRO, Melbourne, Victoria, Australia.

Vanacker, V., A. Molina, G. Govers, J. Poesen, G. Dercon, and S. Deckers (2005), River channel response to short-term human-induced change in landscape connectivity in Andean ecosystems, *Geomorphology*, *72*, 340–353, doi:10.1016/j.geomorph.2005.05.013.

Wainwright, J., and A. J. Parsons (2002), The effect of temporal variations in rainfall on scale dependency in runoff coefficients, *Water Resour. Res.*, *38*(12), 1271, doi:10.1029/2000WR000188.

Wainwright, J., A. J. Parsons, and A. D. Abrahams (2000), Plot-scale studies of vegetation, overland flow and erosion interactions: Case studies from Arizona and New Mexico, *Hydrol. Processes*, *14*, 2921–2943, doi:10.1002/1099-1085(200011/12)14:16/17<2921::AID-HYP127>3.0.CO;2-7.

Western, A. W., G. Blöschl, and R. B. Grayson (2001), Toward capturing hydrologically significant connectivity in spatial patterns, *Water Resour. Res.*, *37*, 83–97, doi:10.1029/2000WR900241.

Wilcox, B. P., D. D. Breshears, and C. D. Allen (2003), Ecohydrology of a resource-conserving semiarid woodland: Effects of scale and disturbance, *Ecol. Monogr.*, *73*, 223–239, doi:10.1890/0012-9615(2003)073[0223: EOARSW]2.0.CO;2.

Wu, X. B., T. L. Thurow, and S. G. Whisenant (2000), Fragmentation and changes in hydrologic function of tiger bush landscapes, south-west Niger, *J. Ecol.*, *88*, 790–800, doi:10.1046/j.1365-2745.2000.00491.x.

———————————

S. Bautista, J. Bellot, and Á. G. Mayor, Departamento de Ecología, Universidad de Alicante, Apdo. 99, E-03080, Alicante, Spain. (ag.mayor@ua.es)

M. Dixon, Foothills Laboratory, University Corporation for Atmospheric Research, 3450 Mitchell Lane, Boulder, CO 80301, USA.

E. E. Small, Department of Geology, University of Colorado, Campus Box 399, 2200 Colorado Ave. Boulder, CO 80309, USA.